UNIVERSITY of York

This is a repository copy of *Icosahedral Carbaboranes with Peripheral Hydrogen–Chalcogenide Groups : Structures from Gas Electron Diffraction and Chemical Shielding in Solution*.

White Rose Research Online URL for this paper:
https://eprints.whiterose.ac.uk/139672/

Version: Accepted Version

Article:
Baše, Tomáš, Holub, Josef, Fanfrlík, Jindřich et al. (7 more authors) (2019) Icosahedral Carbaboranes with Peripheral Hydrogen–Chalcogenide Groups : Structures from Gas Electron Diffraction and Chemical Shielding in Solution. Chemistry : A European Journal. pp. 2313-2321. ISSN 1521-3765

https://doi.org/10.1002/chem.201805145

Reuse
Items deposited in White Rose Research Online are protected by copyright, with all rights reserved unless indicated otherwise. They may be downloaded and/or printed for private study, or other acts as permitted by national copyright laws. The publisher or other rights holders may allow further reproduction and re-use of the full text version. This is indicated by the licence information on the White Rose Research Online record for the item.

Takedown
If you consider content in White Rose Research Online to be in breach of UK law, please notify us by emailing eprints@whiterose.ac.uk including the URL of the record and the reason for the withdrawal request.

White Rose university consortium
Universities of Leeds, Sheffield & York

eprints@whiterose.ac.uk
https://eprints.whiterose.ac.uk/

CHEMISTRY
A European Journal

A Journal of
ChemPubSoc Europe

Accepted Article

Title: Icosahedral carbaboranes with peripheral hydrogen-chalcogenide functions: their structures from gas electron diffraction and chemical shielding in solution

Authors: Norbert Werner Mitzel, Josef Holub, Jindřich Fanfrlík, Drahomír Hnyk, Paul Lane, Derek Wann, Yury Vishnevskiy, Denis Tikhonov, and Christian Reuter

This manuscript has been accepted after peer review and appears as an Accepted Article online prior to editing, proofing, and formal publication of the final Version of Record (VoR). This work is currently citable by using the Digital Object Identifier (DOI) given below. The VoR will be published online in Early View as soon as possible and may be different to this Accepted Article as a result of editing. Readers should obtain the VoR from the journal website shown below when it is published to ensure accuracy of information. The authors are responsible for the content of this Accepted Article.

To be cited as: *Chem. Eur. J.* 10.1002/chem.201805145

Link to VoR: http://dx.doi.org/10.1002/chem.201805145

Supported by
ACES

WILEY-VCH

10.1002/chem.201805145

WILEY-VCH

Icosahedral carbaboranes with peripheral hydrogen-chalcogenide functions: their structures from gas electron diffraction and chemical shielding in solution

Tomáš Baše,[a] Josef Holub,[a] Jindřich Fanfrlík,[b] Drahomír Hnyk,[a*] Paul D. Lane,[c,d] Derek A. Wann,[c] Yury V. Vishnevskiy,[e*] Denis Tikhonov,[e,f,g] Christian G. Reuter[e] and Norbert W. Mitzel[e*]

Abstract: Samples of *closo*-1,2-$(EH)_2$-1,2-$C_2B_{10}H_{10}$ (E = S, Se) have been prepared; in the case of E = Se for the first time. Their semi-experimental equilibrium molecular structures were established by the concerted use of quantum-chemical computations and gas electron diffraction (GED). A method has been developed and implemented to quantify the contribution of experimental data to each refined structural parameter. The accuracy of the experimental structures, as well as those computed at the MP2 level, were gauged by comparison of experimental ^{11}B NMR chemical shifts with quantum-chemically computed ones; the inclusion of electron correlation (GIAO-MP2) provides superior results. For geometrical predictive purposes, the remaining group VI elements were considered and the icosahedral structures for E = O and Te were also computed; for E = O the same theoretical approach was used as for E = S, while for E = Te a similar description as for E = Se was employed.

Introduction

The so-called *ortho*-carborane, *i.e.* 1,2-*closo*-$C_2B_{10}H_{12}$, has received considerable attention in boron cluster chemistry. This neutral molecule is based on a 12-vertex icosahedron with two CH and ten BH vertices. Because $\{CH\}^-$ and $\{BH\}^{2-}$ are isoelectronic units, there are two other structural isomers, differing in the relative positions of the two CH fragments. Of all of these icosahedral clusters, *ortho*-carbaborane is the most intensely studied because its preparation is relatively straightforward. Moreover, it has very rich substitution chemistry. Outer functionalization can be achieved by replacing terminal hydrogen atoms by various substituents to maintain the overall neutral charge. Chalcogen atoms belong to a class of substituents capable of generating derivatives of the icosahedral cage both as part of the cage[1] and as a peripheral group; the latter has so far been exemplified by thiolated carbaboranes. Quite recently it has been found that such compounds form self-assembled monolayers on metal surfaces.[2] *closo*-1,12-$(SH)_2$-1,12-$C_2B_{10}H_{10}$ and *closo*-9,12-$(SH)_2$-1,2-$C_2B_{10}H_{10}$, for example, can act as modifiers of both, gold nanoparticles and gold flat films, due to their strong interaction with coinage metals. Such an affinity of sulfur towards gold, silver and copper is well documented,[3] and often called thiophilic.

Both of these species have been structurally characterized in the solid state[4] and in the gas phase.[5] The rationale for studying the gas-phase structure is that the modification of metal surfaces generally happens from the gas phase. On this basis, we have prepared another known thiolated icosahedral carbaborane, *closo*-1,2-$(SH)_2$-1,2-$C_2B_{10}H_{10}$ (**1**),[6] to expand the gas-phase and structural chemistry of this class of compounds. The affinity of selenium-containing functional groups towards gold, silver and copper surfaces is also substantial. Consequently, we have now attempted to prepare *closo*-1,2-$(SeH)_2$-1,2-$C_2B_{10}H_{10}$ (**2**) as well. It is known that the necessary intermediate for getting **2**, the lithium 1,2-diselenolato-1,2-dicarba-*closo*-dodecaboranate salt $(Li^+)_2$[*closo*-1,2-$(Se)_2$-1,2-$C_2B_{10}H_{10}$]$^{2-}$, tends to dimerize in an oxidative manner[7] and, therefore, could not yet been successfully protonated. The dianion also easily reacts with several silicon compounds.[8]

In the present work the structure of **2** was examined in the gas-phase for the same reason as for **1**. Similarly to sulfur, selenium possesses a much greater scattering ability for electrons than hydrogen and, consequently, the carbaborane core can be characterized in the gas phase more accurately than in the parent *ortho*-carborane.[9] Iodine substitution has also served this purpose.[10]

The tellurium homologue adds to the family of 12-vertex *closo*-systems, and in particular to those containing a group 16 element.[11] 1-$TeB_{11}H_{11}$ has been mentioned in the literature[12] but has so far not been structurally characterized. We have, therefore, computed structural and magnetic properties of 1,2-$(TeH)_2$-1,2-$C_2B_{10}H_{10}$ (**3**) to see whether any of the structural trends along the series S, Se, Te might be reflected in modifying metal surfaces with such chalcogen-functionalized carbaboranes.

[a] Dr. T. Baše, Dr. J. Holub, Dr. D. Hnyk,
Institute of Inorganic Chemistry of the Czech Academy of Sciences,
CZ-250 68 Husinec-Řež, Czech Republic
E-mail:hnyk@iic.cas.cz
[b] Dr. Jindřich Fanfrlík
Institute of Organic Chemistry and Biochemistry of the Czech Academy of Sciences, CZ-166 10 Praha 6, Czech Republic
[c] Dr. P. D. Lane, Dr. D. A. Wann
Department of Chemistry, University of York, Heslington, York, U.K. YO10 5DD
[d] Dr. P. D. Lane, present address:
School of Engineering and Physical Sciences, Heriot-Watt University, Edinburgh, U.K. EH14 4AS.
[e] Dr. Yu. V. Vishnevskiy, Dr. D. Tikhonov, Dr. C. G. Reuter, Prof. Dr. N. W. Mitzel
Fakultät für Chemie, Lehrstuhl für Anorganische Chemie und Strukturchemie, Centrum für molekulare Materialien CM_2,
Universität Bielefeld, Universitätsstr. 25,
33615 Bielefeld, Germany
E-mail: mitzel@uni-bielefeld.de
[f] Dr. D. Tikhonov, present addresses:
M. V. Lomonosov Moscow State University, Department of Physical Chemistry, GSP-1, 1-3 Leninskiye Gory,
119991, Moscow, Russian Federation
[g] FS-SMP Deutsches Elektronen-Synchrotron (DESY),
Notkestrasse 85, Building 25f, Room 353,
22607 Hamburg, Germany

Accepted Manuscript

This article is protected by copyright. All rights reserved.

Results and Discussion

Synthesis

We have achieved a synthesis that yields **2**, an accomplishment that should be appreciated considering that previous attempts to protonate $(Li^+)_2$[*closo*-1,2-$(Se)_2$-1,2-$C_2B_{10}H_{10}]^{2-}$ were not successful and generally led to dimerization; **2** itself is prone to oxidative coupling in air as well (the cyclic eight-membered bis-(diselenane) with annulated carborane moieties is formed). This may be attributed to the higher acidity of **2** in relation to **1**. Generally, organic selenols are much more acidic than thiols.[13] When we computed the gas-phase acidities (GA) of monoacids of **1** and **2** (using the MP2/AE1 method) we found that **2** was slightly more acidic than **1** (1271.4 vs. 1288.2 kJ mol^{-1} for **2** and **1**, respectively). These values are comparable with the value of 1279.5 kJ mol^{-1} GA computed for the monoacid of *closo*-1,2-$(COOH)_2$-1,2-$C_2B_{10}H_{10}$.[14] However, when computing the corresponding GA for the diacids, such values are not so pronounced in terms of GA, which can be ascribed to formation of the CCEH···E pentagonal rings that hinder further deprotonations and suggest that the difficulty in preparing *closo*-1,2-$(EH)_2$-1,2-$C_2B_{10}H_{10}$, particularly for E = Se, is because the Se···H contact is shorter than S···H.

Molecular structure determination by GED

Gas-phase structures of **1** and **2** (Figure 1) have been refined using the program UNEX.[15] In previous studies we have successfully demonstrated the refinement of the molecular structure of 9,12-I_2-*closo*-1,2-$C_2B_{10}H_{10}$ in Cartesian coordinates aided by regularization.[10] The same method has been applied in this work. Quantum-chemical calculations of potential energy surfaces (Figure 2 and 3) revealed a possible existence of two conformations with C_s and C_2 symmetries for both **1** and **2** differing in relative positions of hydrogen atoms. In refinement the geometrical models (see Tables S4 and S5) were constructed so that the symmetries of theoretically predicted conformers were preserved. The functional for minimization had an additional regularization term to stabilize the solution of the inverse problem:

$$Q = Q_{\mathrm{GED}} + \alpha Q_{\mathrm{QC}} = \underbrace{\sum_i \left(s_i M^{\mathrm{model}}(s_i) - s_i M^{\exp}(s_i)\right)^2}_{Q_{\mathrm{GED}}} + \alpha \underbrace{\sum_j \left(p_j^{\mathrm{model}} - p_j^{\mathrm{QC}}\right)^2}_{Q_{\mathrm{QC}}}, \quad (1)$$

where Q_{GED} is the GED discrepancy functional, Q_{QC} is the penalty functional based on the computed quantum-chemical parameters, $sM(s)$ is the reduced molecular scattering intensity, α is the global regularization parameter and p are the refined parameters, in our case Cartesian coordinates. Optimal values for α were determined using a method described recently (see Figures S13–S16).[10]

The compositions of vapors of **1** and **2** were modeled as mixtures of conformations of C_2 and C_s symmetry, which differed mostly in the positions of hydrogen atoms of the -SH and -SeH groups. The contributions of these hydrogen atoms (as atom pairs with all other atoms in the molecules) to the diffraction patterns are, as expected, very small, and refining the conformational composition does not, therefore, lead to meaningful results. Instead, relative amounts of the conformers were calculated from Boltzmann distributions considering MP2/cc-pVTZ energies and temperatures of the corresponding GED experiments. The obtained amounts of the C_2-conformers for **1** and **2** are 55 and 42%, respectively, and were assumed in the structural analysis. Initial refinements were performed using the vibrational amplitudes and distance corrections obtained from MD simulations (models GED-MD, see Tables S6-S9). The MD trajectories projected onto the PES are shown in Figures 2 and 3. After that higher-quality models (denoted as GED-VM) were constructed using vibrational amplitudes and corrections (Tables S10-S13) obtained from quadratic and cubic force fields calculated at the B3LYP/cc-pVTZ level. In refinement of **1** the optimal value of α was found to be 5. In case of **2**, two solutions were found for α = 0.7 and 43. The final refined structural parameters of **1** and **2** are presented in Tables 1 and 2, respectively. The corresponding radial distribution functions are given in Figures 4 and 5.

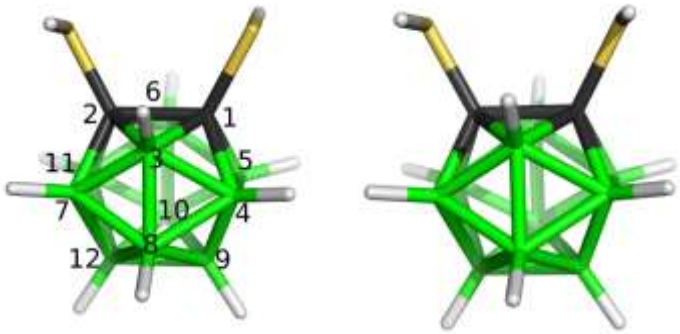

Figure 1. C_2 (left) and C_s (right) conformers of carbaboranedithiole **1** and -selenole **2**, see below.

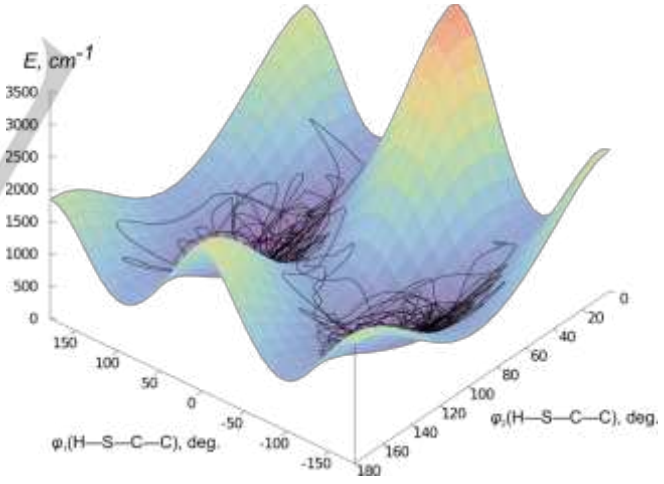

Figure 2. Fragment of PES for **1** with MD trajectory at the B3LYP/6-31G(d) level of theory.

Accepted Manuscript

This article is protected by copyright. All rights reserved.

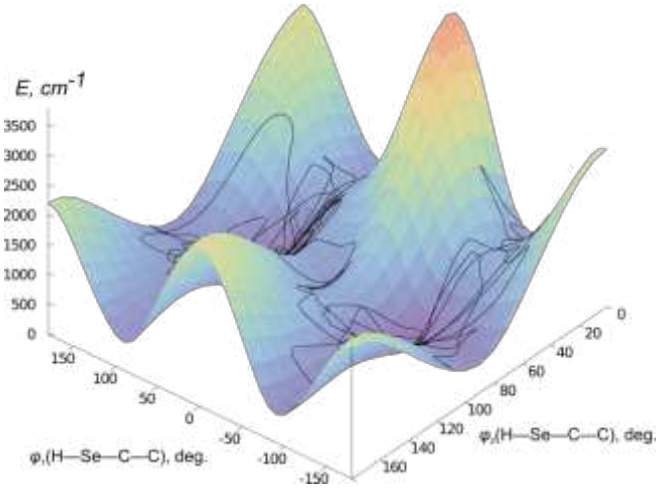

Figure 3. Fragment of PES for **2** with MD trajectory at the B3LYP/6-31G(d) level of theory.

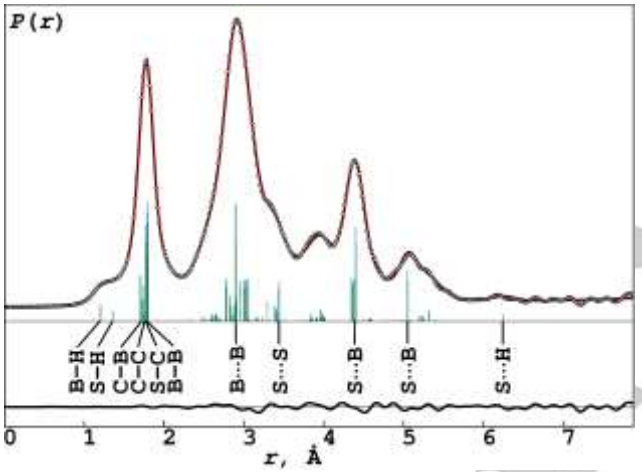

Figure 4. Experimental (circles) and model (solid line) radial distribution functions of **1**. The difference curve is shown at the bottom. Vertical bars indicate the most important interatomic terms.

Table 1. Averaged values of selected theoretical and semi-experimental geometrical parameters (Å, degrees) of **1** with respective experiment contribution factors.[a]

	MP2/cc-pVTZ	GED		
	r_e	r_e	r_g	w^b
*r*B–H	1.181	1.186(5)	1.209(5)	0.00
*r*S–H	1.339	1.341(5)	1.361(5)	0.01
*r*C–B	1.704	1.702(4)	1.722(4)	0.17
*r*C–C	1.756	1.755(7)	1.765(7)	0.08
*r*B–B	1.782	1.777(5)	1.793(5)	0.18
*r*C–S	1.769	1.755(4)	1.770(4)	0.36
∠(C–C–B)$_{narrow}$	59.2	59.2(2)		0.03
∠(C–C–B)$_{wide}$	109.7	109.5(2)		0.02
∠C–B–C	61.5	61.6(2)		0.05
∠(C–B–B)$_{narrow}$	58.3	58.4(2)		0.06
∠(C–B–B)$_{wide}$	105.6	105.7(2)		0.04
∠(B–C–B)$_{narrow}$	63.4	63.3(2)		0.05
∠(B–C–B)$_{wide}$	113.7	113.4(2)		0.10
∠(B–B–B)$_{narrow}$	60.0	60.0(2)		0.04
∠(B–B–B)$_{wide}$	107.9	107.9(2)		0.03
∠S–C–C	118.0	118.0(1)		0.13
∠S–C–B	119.4	119.6(2)		0.07
∠C–S–H	95.4	95.9(2)		0.00
∠C–B–H	116.7	116.7(3)		0.02
∠B–B–H	123.1	123.1(3)		0.01
|∠CCSH(*anti*)|	89.9	89.9(4)		0.00
|∠CCSH(*syn*)|	95.2	95.2(2)		0.00
R_f, %	17.0[c]	5.1		

[a] Averaging was done for parameters of the same type both in C_2- and C_s-conformers. Numbers in parentheses are standard deviations obtained in least squares analysis.

[b] Contribution of experimental GED data into parameters.

[c] For the model with respective theoretical molecular structure.

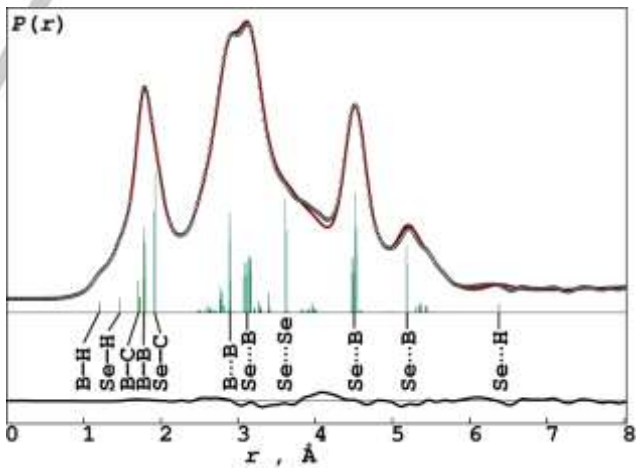

Figure 5. Experimental (circles) and model (solid line) radial distribution functions of **2**. The difference curve is shown at the bottom. Vertical bars indicate the most important interatomic terms.

Accepted Manuscript

This article is protected by copyright. All rights reserved.

Table 2. Averaged values of selected theoretical (MP2/cc-pVTZ) and semi-experimental geometrical parameters (Å, degrees) of **2** with respective experiment contribution factors.[a]

	MP2	GED				
	r_e	α = 0.7		α = 43		
	r_e	r_e	w^b	r_e	r_g	w^b
*r*B–H	1.181	1.197(20)	0.15	1.188(4)	1.209(4)	0.00
*r*Se–H	1.454	1.508(17)	0.39	1.457(4)	1.475(4)	0.02
*r*C–B	1.705	1.689(17)	0.94	1.699(3)	1.720(3)	0.24
*r*C–C	1.731	1.750(28)	0.93	1.726(5)	1.725(5)	0.17
*r*B–B	1.782	1.777(19)	0.94	1.775(3)	1.790(3)	0.24
*r*C–Se	1.904	1.902(10)	0.99	1.904(3)	1.922(3)	0.52
∠(C–C–B)$_{narrow}$	59.7	59.1(8)	0.82	59.7(1)		0.10
∠(C–C–B)$_{wide}$	110.0	109.6(8)	0.87	109.9(1)		0.08
∠C–B–C	60.6	61.8(10)	0.93	60.6(2)		0.15
∠(C–B–B)$_{narrow}$	58.3	58.2(7)	0.91	58.4(1)		0.12
∠(C–B–B)$_{wide}$	105.3	105.8(9)	0.83	105.3(2)		0.07
∠(B–C–B)$_{narrow}$	63.3	63.6(7)	0.89	63.3(1)		0.10
∠(B–C–B)$_{wide}$	114.0	113.8(8)	0.95	114.0(2)		0.22
∠(B–B–B)$_{narrow}$	60.0	60.0(7)	0.76	60.0(1)		0.06
∠(B–B–B)$_{wide}$	107.9	107.8(9)	0.77	107.9(2)		0.05
∠Se–C–C	119.2	119.2(4)	0.97	119.3(1)		0.32
∠Se–C–B	118.9	119.1(9)	0.91	118.9(2)		0.17
∠C–Se–H	93.9	93.1(9)	0.03	94.0(2)		0.00
∠C–B–H	117.0	117.8(12)	0.75	117.1(2)		0.04
∠B–B–H	123.1	123.0(12)	0.51	123.1(2)		0.02
|∠CCSeH(*anti*)|	84.7	83.2(16)	0.04	84.6(3)		0.00
|∠CCSeH(*syn*)|	92.1	93.9(7)	0.24	92.7(1)		0.00
R_f, %	10.8[c]	4.0		5.1		

[a] Averaging was done for parameters of the same type both in C_2- and C_s-conformers. Numbers in parentheses are standard deviations obtained in least squares analyses.

[b] Contribution of experimental GED data into parameters.

[c] For the model with respective theoretical molecular structure.

Contribution of experimental data to refined structures

As described above, stable least-squares refinements of structures of **1** and **2** based on GED data could be performed using additional information from quantum-chemical calculations. In this sense the resulting structures are semi-experimental. Accordingly, an important question can be raised: to what extent can the structures be considered experimental? Recently we have already formulated this problem and developed a simple numerical method for its solving.[16] However, the proposed procedure was essentially empirical. In the present work we have developed a more advanced and theoretically sound method.

Let us consider a minimization of a least-squares functional Q based on multiple data sets:

$$Q = \sum_i Q_i \rightarrow min,$$

where Q_i denotes the discrepancy functional for the i-th data set. Our goal is to build a function w_i which characterizes the contribution of the i-th data set to refined parameters. This function should satisfy the following conditions: $w_i \in [0;1]$ and $\sum_i w_i = 1$. The functional Q can be approximated using a Taylor expansion in the vicinity of the minimum:

$$Q \approx \sum_i \left(\begin{array}{c} Q_i^{\min} + \sum_n \left(\frac{\partial Q_i}{\partial x_n}\right)_{\min} (x_n - x_n^{\min}) + \\ + \frac{1}{2}\sum_n \sum_m \left(\frac{\partial^2 Q_i}{\partial x_n \partial x_m}\right)_{\min} (x_n - x_n^{\min})(x_m - x_m^{\min}) + \cdots \end{array} \right),$$

where x_m and x_n are refined parameters, min denotes the minimum of Q. Cross-terms can be ignored if the correlations between parameters are small. In this case

$$Q \approx \sum_n q_n,$$

where q_n is the part of total functional depending only on parameter x_n, which can be further represented as a sum (below we omit subscript n for clarity):

$$q = \sum_i q_i \approx \sum_i \left(a_0^{(i)} + a_1^{(i)}\left(x - x^{\min}\right) + \frac{a_2^{(i)}}{2}\left(x - x^{\min}\right)^2 + \cdots \right),$$

where q_i is the partial functional for the i-th data set,

$$a_k^{(i)} = \left(\frac{\partial^k Q_i}{\partial x^k}\right)_{min}.$$

The functional q can be associated with a probability distribution p as $q = -\ln(p) + \text{const}$. Obviously $p \propto \prod_i p_i$, where p_i is the partial distribution corresponding to the functional q_i. Taking only the first three terms of the expansion for q_i the distribution p_i is a Gaussian function

$$p_i = \frac{1}{\sigma_i \sqrt{2\pi}} \exp\left(\frac{-(x - \mu_i)^2}{2\sigma_i^2}\right)$$

with a dispersion $\sigma_i^2 = 1/a_2^{(i)}$ and a mean $\mu_i = -a_1^{(i)}/a_2^{(i)}$. A possible way of defining ω_i is through the measure of proximity of the dispersion of p_i to the dispersion of the total p. It is simple to show that the following equality is true:

$$\frac{1}{\sigma^2} = \sum_i \frac{1}{\sigma_i^2}$$

Accepted Manuscript

This article is protected by copyright. All rights reserved.

Therefore it is possible to define the measure of contribution of the *i*-th functional in the parameter *x* as:

$$w_i = \frac{\sigma^2}{\sigma_i^2} = \frac{a_2^{(i)}}{\sum_j a_2^{(j)}},$$

where the summation in the denominator is performed for all data sets Q_i. This expression can be directly used for independently refined parameters. It is also valid for dependent parameters ξ; however, the corresponding second derivatives a_2 should additionally be evaluated as:

$$\left(\frac{\partial^2 Q_i}{\partial \xi^2}\right)_{\min} = \sum_n \sum_m \left(\frac{\partial^2 Q_i}{\partial x_n \partial x_m}\right)_{\min} \left(\frac{\partial x_n}{\partial \xi}\right)\left(\frac{\partial x_m}{\partial \xi}\right) + \sum_n \left(\frac{\partial Q_i}{\partial x_n}\right)_{\min} \left(\frac{\partial^2 x_n}{\partial \xi^2}\right).$$

For the geometrical parameters the second derivatives

$$\left(\frac{\partial^2 x_n}{\partial \xi^2}\right)$$

are small and therefore the second term of the expression can be omitted to a good approximation.

Molecular geometries from GED

Tables 1 and 2 list the averaged values of the most important geometric parameters of **1** and **2**, respectively, refined from GED data with inclusion of required portion of regularization. These values are compared to quantum-chemically calculated ones. The computed contributions of GED data to the refined parameters (*w* in Tables 1 and 2) show that parameters defining the hydrogen positions are in fact mostly theoretical. Without having values of *w* it could be mistakenly believed that GED can determine positions of hydrogens in **1** and **2** with a precision of several thousands of an Angstrom on an experimental basis.

The values of *w* for the B–B, B–C and C–C bonds are experimental only to about 10–25%. The bonds C–S and C–Se are those with the biggest experimental contribution with *w* = 36 and 52%, respectively. This agrees well with common qualitative expectations about so-called strong and weak parameters in GED refinements. However, the proposed method for calculation of *w* values is probably not the only possible way for numerical expression of contributions of experimental data to refined parameters. Therefore the absolute values of *w* should be assessed with caution. It is more reliable to compare *w* values for different parameters within one molecule or for the same parameters in a molecule obtained from refinements with different extent of regularization. In case of **1** and **2** geometrical parameters were refined independently (without fixed constraints) and were all regularized to the same extent; that is, there were no different individual weights in the second term of the functional shown in equation 1. The regularization was controlled only by the single global parameter α. This was done in order to keep the natural relationship between weak and strong parameters in GED and to show this explicitly in the final results.

The other interesting aspect is the influence of the global regularization parameter α on the contribution of experimental data into refined parameters. Obviously, in the case where $\alpha = 0$ the parameters are completely experimental, but under these conditions the solution of the problem becomes very unstable yielding unphysical values. In the opposite case, when α approaches infinity, experimental GED intensities play no role and the parameters are refined effectively only on the basis of theoretical data and approach exactly the regularization values.

In the refinement of **2** we found two solutions (represented in Table 2) with different values for α. In the case of $\alpha = 0.7$ the contribution of experimental GED data in the parameters approaches 90–100%, except for parameters defining hydrogen positions. However, the standard deviations of the refined parameters were relatively large. This is the price for refining all the parameters without fixed constraints and applying only a very small portion of regularization. In contrast, the second stable solution with $\alpha = 43$ showed systematically lower *w*'s but also smaller standard deviations and correlations. Naturally, the agreement with experimental data in this case was also somewhat worse, as the *R* factors show. The first solution had relatively large deviations from regularization values, at least for Se–H and C–C bond lengths. Thus, the case for $\alpha = 0.7$ was considered as on the border of stability and as the main solution was chosen the second case $\alpha = 43$. Also this second solution gave parameters with contributions of experimental GED data comparable to those from the refinement of **1**. This is expected since both molecules are similar from GED point of view, which can be seen by comparing their radial distribution functions (Figures 4 and 5).

Table 4 C–C bond lengths in Å for all the compounds considered for the selected geometries.

	O		S (**1**)		Se (**2**)		Te (**3**)	
	C_2	C_s	C_2	C_s	C_2	C_s	C_2	C_s
MP2/AE1	1.773	1.779	1.754	1.758	1.727	1.735		
MP2/AE2	1.726	1.728	1.740	1.750				
MP2/AE3					1.724	1.741		
MP2/AE4					1.732	1.743		
MP2/ECP1					1.732	1.742	1.715	1.727
MP2/ECP2					1.729	1.735	1.712	1.721
GED			1.753(7)	1.757(7)	1.724(5)	1.728(5)		

Accepted Manuscript

This article is protected by copyright. All rights reserved.

Comparison of the final refined structures of **1** and **2** at first sight revealed stability of the boron part of molecular cage: averaged B–B distances and B–B–B angles are very similar in both molecules. However, inspection of *w* values clearly indicated that this result was mostly dictated by theory due to applied regularization. Indeed, the contribution of GED data to B–B distances was about 20%, for the B–B–B angles it was even lower, about 3-5%. Fortunately, for **2** we had another refinement with low α. The B–B distances and B–B–B angles in this refinement had much larger contributions from experiment, up to 94%, but nearly the same values as in the main model. Thus, we observed stability of the refined values of these parameters with respect to regularization and could assume the same stability in case of **1** due to the same type of structure. This made us to conclude that GED experiment still proved the equality of purely boron parts of structures in **1** and **2** within indicated uncertainties.

Somewhat worse was situation with the C–C bonds. Table 2 shows that the refined value of the C–C bond length can be unstable with weak regularization, its values largely differed for solutions with α = 0.7 and α = 43. In the final models of **1** and **2** the refined values of the C–C bond length were significantly different, r_e = 1.755(7) and 1.726(5) Å, respectively. However, they were determined with relatively low contributions of experimental data, 8 and 17%, respectively. Thus, it was not possible to determine with great confidence the difference between C–C bond lengths in **1** and **2**.

The structures in which E = O, Te were also tackled but only computationally to enable us to compare the C–C distances in the whole series of 1,2-$(EH)_2$-1,2-$C_2B_{10}H_{10}$ (see Table 4): the heavier the chalcogen atom is, the shorter the C–C distance in the carbaborane core, which is probably one of the most interesting structural results obtained from this series of compounds. If the C–C bond length in the gas-phase structure in **1** is one of the driving forces in the modification of various metal surfaces, **2** might behave in similar manner in this respect, possibly on the basis of close C–C distances of the carbaborane core when comparing **1** and **2**.

Table 3 Calculated and experimental (in $CDCl_3$) ^{11}B NMR chemical shifts for *closo*-1,2-$(EH)_2$-1,2-$C_2B_{10}H_{10}$, E = S (**1**), Se (**2**), Te (**3**).[a]

	$\delta(^{11}B)$ / ppm			
	B(3,6)[b]	B(4,5,7,11)	B(8,10)[b]	B(9,12)
	1			
GIAO-MP2/IGLO-II//MP2/AE2 C_2	−7.6	−6.5	−9.4	−3.1
GIAO-MP2/IGLO-II//MP2/AE2 C_s	−8.9(−5.3/−12.5)	−6.3	−8.6(−7.9/−9.3)	−3.3
GIAO-MP2/IGLO-II//GED C_2	−7.7	−6.7	−9.4	−3.0
GIAO-MP2/IGLO-II//GED C_s	−8.2(−4.5/−11.9)	−6.6	−8.9(−8.0/−9.7)	−3.2
ZORA-BP86(SO)/TZP//MP2/AE2 C_2	−13.5	−11.9	−14.6	−6.9
ZORA-BP86(SO)/TZP//MP2/AE2 C_s	−14.7(−10.7/−18.6)	−11.4	−13.7(−12.8/−14.6)	−7.2
ZORA-BP86(SO)/TZP// GED C_2	−13.5	−11.9	−14.5	−6.9
ZORA-BP86(SO)/TZP// GED C_s	−13.9(−9.9/−18.0)	−11.7	−14.0(−12.9/−15.1)	−7.2
Experimental[c]	−10.6	−8.5	−10.6	−4.5
	2			
GIAO-MP2/AE5//MP2/AE3 C_2	−6.5	−5.9	−8.4	−1.9
GIAO-MP2/AE5//MP2/AE3 C_s	−8.1(−4.5/−11.7)	−5.5	−7.5(−6.6/−8.5)	−2.0
GIAO-MP2/AE5//MP2/AE4 C_2	−6.9	−5.9	−8.2	−1.9
GIAO-MP2/AE5//MP2/AE4 C_s	−8.1(−4.5/−11.7)	−5.5	−7.4(−6.5/−8.3)	−2.0
GIAO-MP2/AE5//MP2/ECP1 C_2	−7.0	−5.9	−8.1	−2.0
GIAO-MP2/AE5//MP2/ECP1 C_s	−8.2(−4.6/−11.8)	−5.5	−7.3(−6.5/−8.1)	−2.1
GIAO-MP2/AE5//GED C_2	−7.2	−6.1	−8.7	−2.6
GIAO-MP2/AE5//GED C_s	−8.5(−4.9/−12.0)	−6.2	−7.7(−6.8/−8.6)	−2.4
ZORA-BP86(SO)/TZP//MP2/AE3 C_2	−12.1	−11.3	−13.4	−6.1
ZORA-BP86(SO)/TZP//MP2/AE3 C_s	−13.6(−9.3/−18.0)	−10.7	−12.6(−11.3/−13.9)	−6.2
ZORA-BP86(SO)/TZP//MP2/AE4 C_2	−12.4	−11.2	−13.2	−6.1
ZORA-BP86(SO)/TZP//MP2/AE4 C_s	−13.6(−9.3/−17.9)	−10.8	−12.4(−11.8/−13.7)	−6.2
ZORA-BP86(SO)/TZP//MP2/ECP1 C_2	−12.6	−11.2	−13.1	−6.2
ZORA-BP86(SO)/TZP//MP2/ECP1 C_s	−13.7(−9.4/−18.0)	−10.8	−12.3(−11.1/−13.5)	−6.2
Experimental[c]	−9.2	−8.2	−9.2	−3.7
	3			
GIAO-MP2/ECP3//MP2/ECP2 C_2	−6.4	−4.9	−6.6	−3.2
GIAO-MP2/ECP3//MP2/ECP2 C_s	−7.7(−4.4/−10.9)	−4.6	−6.0(−5.0/−7.1)	−2.5
ZORA-BP86(SO)/TZP//MP2/ECP2 C_2	−11.6	−10.4	−10.6	−3.8
ZORA-BP86(SO)/TZP//MP2/ECP2 C_s	−12.8(−9.1/−16.5)	−10.0	−10.0(−8.5/−11.5)	−3.6

[a] Relative to $BF_3{\cdot}OEt_2$; see text for description and Figure 1 for atom numbering. [b] As the values for B(3) and B(6) and B(8) and B(10) differ significantly for the calculated structures in the C_s values, giving only the average may be misleading, hence the individual values for B(3)/B(6) and B(8)/B(10) are also given in parentheses for these structures. [c] This work, which also includes the computed ^{11}B NMR for E = O, see Table S26. Similarly as for **1**, just three signals were experimentally detected, with the intensities 4:4:2 (*i.e.* (2+2):4:2). The ^{77}Se NMR chemical shift is 367 ppm, the computed mean value obtained at the GIAO-MP2/AE5//MP2/AE4 level is 291 ppm.

Accepted Manuscript

This article is protected by copyright. All rights reserved.

NMR computations

Table 3 reveals a very good accord between the calculated and experimental ^{11}B chemical shifts using the GIAO-MP2 model chemistry based on various MP2 geometries including GED ones; the latter did not have a pronounced influence on the computed results. Inspection of the table confirms such a conclusion. The ADF code performs worse in this respect; it tends to exaggerate shieldings of all boron atoms systematically with respect to experimental data (to lower frequencies). This is the effect of dynamic electron correlation that makes the GIAO-MP2 approach superior to the ZORA approach. It is quite apparent that neither S nor Se have significant influence on the ^{11}B NMR chemical shifts with respect to the parent compound, see also ref. 5b. Table 3 also shows a good accord between the computed and experimental ^{77}Se chemical shifts, which further supports the correctness of the molecular structure of **2** in the liquid phase.

Chalcogen atoms are further away from the boron core and C–S(Se) bonds exhibit predominantly p-character (at MP2/AE5). This means that no large spin-orbit corrections (SO) are to be expected for calculations of the ^{11}B magnetic shieldings in terms of ZORA approach, since such effects are usually transmitted *via* a Fermi-contact-type relay mechanism. This is very efficient when bonds with high s character are involved,[17] as was also found for *arachno*-$Se_2B_8H_{10}$[18] and *closo*-1-$SeB_{11}H_{11}$,[1] where chalcogen atoms are much closer with respect to the boron arrangement. The explicit ZORA-BP86(SO) approach unambiguously confirmed this expectation since estimated scalar ZORA values from those shown in Table 3 just by subtracting SO contributions were almost the same as ZORA-BP86(SO) reported in this table.

Therefore relativistic effects do not need to be considered seriously for E = S and Se. Larger deviations from the experimental values are achieved through the use of the BP86 functional from the reason mentioned above.

Conclusions

Although **1** has been known for decades, **2** was only obtained as part of this current work, which enriches the body of *exo*-substituted carbaboranes available. Both structures were determined by using the GED and *ab initio*/GIAO/NMR method,[19] quite often used in structural chemistry of boron clusters since the solid-state structural studies are hindered by disordered single-crystals. A new method for calculation of contributions *w* of experimental GED data to refined parameters significantly improves the quality assessment of refined parameters and realistic possibilities of GED method. Taking the C–Se bond in **2** as an example we see that the difference between refined and theoretical values correlates very weakly with *w*. This can be interpreted in a way that this bond length in **2** is a "good" parameter for the GED method, i.e. its value is stably refined independent on the extent of regularization. Taking into consideration that the difference itself is very small we can also conclude that the theoretical value is accurate. Overall, the presented gas-phase structures of **1** and **2** reveal that the positions of C–S and C–Se distances in the corresponding radial distribution curves in which chalcogens are involved are unambiguously determined, which is in line with the gas-phase structures of *closo*-1-$SB_{11}H_{11}$ and *closo*-1-$SeB_{11}H_{11}$[1] and helps to determine the carbaborane moiety relatively accurately. The gas-phase structures of **1** and **2** are in good accord with various MP2 geometries as comparison between the measured and computed ^{11}B NMR spectra revealed. The agreement between the computed and experimental ^{77}Se NMR spectra is also good, considering the fact that the chemical shift range for δ(Se) is 3000 ppm.[45] The experimental EH functionalization of other *closo* carbaboranes is in progress.

Experimental Section

Syntheses

***closo*-1,2-$(SH)_2$-1,2-$C_2B_{10}H_{10}$ (1).** The sample (purity >98% as assessed by GC MS) was prepared according to a literature procedure[6] and purified by chromatography through a silica gel column, followed by crystallization from a hot mixture of hexane and dichloromethane (1:1).

***closo*-1,2-$(SeH)_2$-1,2-$C_2B_{10}H_{10}$ (2).** In analogy with the known synthesis of **1**, butyl lithium (3 ml of a 1.6 M solution in hexane, 4.8 mmol) was added to a solution of *ortho*-carborane (0.34 g, 2.4 mmol) in diethyl ether (50 ml) at room temperature. A white suspension was obtained and stirred for 2 h. Addition of selenium (0.37 g, 4.7 mmol) gave, after 24 h, a yellow solution. The reaction mixture was next cooled to 0 °C and a solution of 20 ml of anhydrous trifluoroacetic acid was added. After stirring at room temperature for 15 min., the ether layer was separated, dried over magnesium sulfate and evaporated to dryness, yielding 0.65 g of crude **2**, which was recrystallized from pentane and then sublimed as a yellowish powder. The yield of pure compound (0.55 g) was 78%, based on starting *ortho*-carborane. Its purity >98% was assessed by GC MS. Again, its architecture was verified by ^{11}B NMR and ^{77}Se spectroscopies, including two-dimensional *COSY* (*CO*rrelated *S*pectroscop*Y*) measurements for the first spectra, see Table 3.

Computational methods

Calculations were performed using the resources provided by the EPSRC UK National Service for Computational Chemistry Software (NSCCS) at Imperial College London and Computing Centre at the University of Köln running the Gaussian 09 suite of programs[20] and Amsterdam Density Functional (ADF)[21] code running at the University of York.

Molecular structures and gas-phase acidities. Gaussian 09 was used to perform 2-D scans of potential energy along two CCXH (X = S, Se) torsion angles for each of **1** and **2**, revealing stable structures of C_s and C_2 symmetry (see Figures 2 and 3). Two conformations belonging to these point groups have also been identified in geometry optimizations of **3**. With these symmetry constraints, geometries were optimized using the MP2[22] method to include the energy due to electron correlation. All MP2 calculations were spin restricted and with frozen core, using one of the following all-electron (AE) basis-set combinations: for **1** cc-pVTZ on all atoms (AE1), 6-31+G(d) on all atoms (AE2); for **2** 641(d) on Se and 6-31+G(d) on B, C and H (denoted AE3), 962(d) on Se and 6-31+G(d)[23] on B, C and H (denoted AE4). The 641(d) and 962(d) basis sets for Se are Binning and Curtiss' [6s4p1d] contraction[24] of Dunning's (14s11p5d)

Accepted Manuscript

This article is protected by copyright. All rights reserved.

primitive set.[25] These basis-set combinations have performed very well for similar types of molecules.[18]

Additional calculations were performed using the quasi-relativistic Stuttgart-Dresden effective core potential (ECP)[26] for Se and Te with polarized double-zeta valence basis set augmented with a diffuse sp set[27] and a d polarization function,[28] together with 6-31+G(d) basis on B, C and H (denoted ECP1) for **2** and **3**; SDB-cc-pVTZ[29] on Se and Te and cc-pVTZ on C, B, H (denoted as ECP2) were also used for **2** and **3.** Gas-phase acidity results are from second derivative analyses performed at the MP2/AE1 level and are defined as the difference in free energies between that of a neutral species and the sum of those of an anion and H^+.

Gas electron diffraction (GED). Electron diffraction patterns were recorded on the recently improved Balzers Eldigraph KDG2 gas electron diffractometer[30] at Bielefeld University. Data for **1** and **2** were collected at two different nozzle-to-detector distances, namely 250.0 and 500.0 mm, with the samples heated to 409±4 K. Experimental conditions are presented in Table S1 of the Supporting Information. Electron diffraction patterns were measured on Fuji BAS IP MP imaging plates, which were scanned using a calibrated Fuji BAS 1800II scanner. The respective total intensity curves (Tables S2 and S3 and Figures S1–S6 in SI) were obtained by applying the method described in elsewhere.[31] Electron wavelengths were refined as is routine[32] using diffraction patterns of CCl_4, recorded along with the substances under study.

Vibrational amplitudes and corrections. For the refinements of the molecular structures of **1** and **2** from GED data vibrational amplitudes and corrections (r_a–r_e) have been computed for all pairs of atoms. One set of these parameters has been calculated using standard perturbation theory formulated by Sipachev[33] and implemented in the VibModule program.[34] Precomputed at the B3LYP/cc-pVTZ level geometry, analytical harmonic and numerical cubic force fields have been utilized in this procedure. For testing purposes another set of parameters has been calculated using molecular dynamics (MD) simulations and applying additional quantum corrections computed with our newly developed program Qassandra.[35] The MD trajectories were obtained using the GAMESS US software[36] at the B3LYP/6-31G(d) level of theory. The simulations for both compounds were started from stable structures of C_s and C_2 symmetry and were carried out for the temperature of GED experiment using chains of two Nosé-Hoover NVT thermostats. The trajectory lengths were 2.5 ps and 1.9 ps for **1** and **2**, respectively, with a time step of 0.2 fs for all simulations. The first 0.4 ps of the trajectories were ignored to account for the equilibration phase.

Magnetic shielding calculations. Magnetic shieldings were calculated using the GIAO-MP2 method[37] implemented within the Gaussian 09 suite of programs. The IGLO-II basis set[38] was used throughout for S, B, C and H atoms, together with one of the following basis sets for Se: 962+(d)[39] (denoted AE5), the abovementioned ECP with its augmented valence basis and (denoted ECP3), and IGLO-II without f functions[40] (denoted II') and only with ECP3 for Te. MP2/AE1 geometries were not used for the computations of magnetic shieldings.

Additional NMR calculations were performed using the MP2/AE5 optimized geometry with the Amsterdam density functional (ADF) code[21] employing the BP86 functional.[41] The two-component relativistic zeroth-order regular approximation (ZORA) method[42] including scalar and spin-orbit (SO)[43] corrections were employed for these computations. We have used the triple-zeta basis set plus one polarization function (denoted TZP; from the ADF library) for all atoms. ^{11}B chemical shifts were calculated relative to B_2H_6 and converted to the usual $BF_3{\cdot}OEt_2$ scale using the experimental $\delta(^{11}B)$ value for B_2H_6 of 16.6 ppm.[44] NMR chemical shifts are given in Table 3.

Electronic supplementary information (ESI) available

Experimental ED conditions (Table S1), intensity data (Tables S2 and S3 and Figures S1–S6), geometrical models (Tables S4 and S5), vibrational amplitudes and distance corrections (Tables S6–S13).Tables S14-S22 list the Cartesian geometries of **1** and **2**, whereas Table S23 provides scale factors from GED refinements and Table S24-S24 show correlation matrices from these procedures. Table S26 gives computed ^{11}B NMR chemical shifts for E = O. Characteristic curves for the regularization parameter α are given in Figures S13-S16.

Keywords: carbaboranes • thioles • selenoles • gas-phase electron diffraction • quantum-chemical calculations • method development

Acknowledgements

This work was supported by Deutsche Forschungsgemeinschaft (DFG, grant MI477/22-1 and core facility GED@BI, grant MI477/35-1). Yu. V. V. is grateful to DFG (grant VI 713/1-2, project number 243500032) for financial support and to HPC facilities at the Universität zu Köln for providing computational time and programs. Financial Support from Czech Science Foundation (project No 17-08045S) is also appreciated. DAW and PDL thank the EPSRC for funding (EP/I004122). We also thank Dr. O. L. Tok for measuring ^{77}Se NMR spectra.

[1] Electron-diffraction structure of *closo*-1-$SB_{11}H_{11}$: (a) D. Hnyk, E. Vajda, M. Bühl, P.v.R. Schleyer, *Inorg. Chem.*, **1992**, *31*, 2464; (b) MW structure of *closo*-1-$SB_{11}H_{11}$: H. Møllendal, S. Samdal, J. Holub, D. Hnyk, *Inorg. Chem.*, **2003**, *42*, 3043; (c) Electron-diffraction structure of *closo*-1-$SeB_{11}H$: D. Hnyk, D. A. Wann, J. Holub, M. Bühl, H. E. Robertson, D. W. H. Rankin, *Dalton Trans.*, **2008**, 96-100.

[2] (a) T. Baše, Z. Bastl, Z. Plzák, T. Grygar, J. Plešek, M. J. Carr, V. Malina, J. Šubrt, J. Boháček, E. Večerníková, O. Kriz, *Langmuir*, **2005**, *21*, 7776; (b) J. N. Hohman, P. P. Zhang, E. I. Morin, P. Han, M. Kim, A. R. Kurland, P. D. McClanahan, V. P. Balema, P. S. Weiss, *ACS Nano*, **2009**, *3*, 527; (c) J. N. Hohman, S. A. Claridge, M. Kim, P. S. Weiss, *Mat. Sci. Eng. R.*, **2010**, *70*, 188; (d) J. C. Thomas, D. P. Goronzy, A. C. Serino, H. S. Auluck, O. R. Irving, E. Jimenez-Izal, J. M. Deirmenjian, J. Macháček, P. Sautet, A. N. Alexandrova, T. Baše, P. S. Weiss, *ACS Nano*, **2018**, *12*, 2211.

[3] See, for example, C. Vericat, M. E. Vela, G. Benitez, P. Carro, E. C. Salvarezza, *Chem. Soc. Rev.*, **2010**, *39*, 1805.

[4] T. Baše, Z. Bastl, M. Šlouf, M. Klementová, J. Šubrt, A. Vetushka, M. Ledinský, A. Fejfar, J. Macháček, M. J. Carr, M. G. S. Londesborough, *J. Phys. Chem. C*, 2008, ***112***, 14446.

[5] (a) Using gas electron diffraction along with *ab initio* calculations provided the structure of 1,12-$(SH)_2$-1,2-$C_2B_{10}H_{10}$: D. Hnyk, J. Holub, M. Hofmann, P. v. R. Schleyer, H. E. Robertson, D. W. H. Rankin, *J. Chem. Soc., Dalton Trans.*, **2000**, 4617; (b) The same kind of the structure for the 9,12-$(SH)_2$-derivative is reported in D. A. Wann, P. D. Lane, H. E. Robertson, T. Baše, D. Hnyk, *Dalton Trans.*, **2013**, *42*, 12015.

Accepted Manuscript

This article is protected by copyright. All rights reserved.

[6] See, for example, F. Teixidor, R. W. Rudolph, *J. Organomet. Chem.*, **1983**, *241*, 301.
[7] B. Wrackmeyer, Z. G. Hernández, R. Kempe, M. Herberhold, *Eur. J. Inorg. Chem.*, **2007**, 239.
[8] B. Wrackmeyer, E. V. Klimkina, W. Milius, *Appl. Organometal. Chem.*, **2010**, *24*, 25.
[9] A. R. Turner, H. E. Robertson, K. B. Borisenko, D. W. H. Rankin, M. A. Fox, *Dalton Trans.*, **2005**, 1310, and references therein.
[10] Yu. V. Vishnevskiy, D. T. Tikhonov, C. G. Reuter, N. W. Mitzel, D. Hnyk, J. Holub, D. A. Wann, P. D. Lane, R. J. F. Berger, S. A. Hayes, *Inorg. Chem.*, **2015**, *54*, 11868.
[11] Review: K. Vyakaranam, J. A. Maguire, N. S. Hosmane, *J. Organomet. Chem.*, **2002**, *646*, 21.
[12] The insertion of Te into a boron cluster is mentioned in G. D. Friesen, L. J. Todd, *J. Chem. Soc., Chem. Commun.*, **1978**, 349.
[13] L. A. Wessjohann, A. Schneider, M. Abbas, W. Brandt, *Biol. Chem.*, **2007**, *388*, 997-1006.
[14] J. M. Oliva-Enrich, S. Humbel, J. A. Santaballa, I. Alkorta, R. Notario, J. Z. Davalos, M. Canle-L, E. Bernhardt, J. Holub, D. Hnyk, *ChemistrySelect*, **2018**, *3*, 4344-4353.
[15] Yu. V. Vishnevskiy, UNEX 1.6, http://unexprog.org.
[16] D. S. Tikhonov, Yu. V. Vishnevskiy, A. N. Rykov, O. E. Grikina, L. S. Khaikin, *J. Mol. Struct.*, **2017**, 1132, 20–27.
[17] M. Kaupp, O. L. Malkina, V. G. Malkin, P. Pykkö, *Chem. Eur. J.*, **1998**, *4*, 118.
[18] D. Hnyk, M. Bühl, J. Holub, S. A. Hayes, D. A. Wann, I. D. Mackie, K. B. Borisenko, H. E. Robertson, D. W. H. Rankin, *Inorg. Chem.*, **2006**, *45*, 6014.
[19] D. Hnyk, D. A. Wann, in *Boron: The Fifth Element*, Vol. 20, Springer, Dordrecht, **2015**, pp. 17 – 48.
[20] M. J. Frisch, G. W. Trucks, H. B. Schlegel, G. E. Scuseria, M. A. Robb, J. R. Cheeseman, G. Scalmani, V. Barone, B. Mennucci, G. A. Petersson, H. Nakatsuji, M. Caricato, X. Li, H. P. Hratchian, A. F. Izmaylov, J. Bloino, G. Zheng, J. L. Sonnenberg, M. Hada, M. Ehara, K. Toyota, R. Fukuda, J. Hasegawa, M. Ishida, T. Nakajima, Y. Honda, O. Kitao, H. Nakai, T. Vreven, J. A. Montgomery, Jr., J. E. Peralta, F. Ogliaro, M. Bearpark, J. J. Heyd, E. Brothers, K. N. Kudin, V. N. Staroverov, R. Kobayashi, J. Normand, K. Raghavachari, A. Rendell, J. C. Burant, S. S. Iyengar, J. Tomasi, M. Cossi, N. Rega, J. M. Millam, M. Klene, J. E. Knox, J. B. Cross, V. Bakken, C. Adamo, J. Jaramillo, R. Gomperts, R. E. Stratmann, O. Yazyev, A. J. Austin, R. Cammi, C. Pomelli, J. W. Ochterski, R. L. Martin, K. Morokuma, V. G. Zakrzewski, G. A. Voth, P. Salvador, J. J. Dannenberg, S. Dapprich, A. D. Daniels, Ö. Farkas, J. B. Foresman, J. V. Ortiz, J. Cioslowski, D. J. Fox, Gaussian 09, revision D.01, Gaussian, Inc., Wallingford CT, **2009**.
[21] (a) E. J. Baerends, D. Ellis, P. Ros, *Chem. Phys.*, **1973**, *2*, 41; (b) G. te Velde, E. J. Baerends, *J. Comput. Phys.*, **1992**, *99*, 84; (c) C. Fonseca Guerra, J. G. Snijders, G. te Velde, E. J. Baerends, *Theor. Chim. Acta*, **1998**, *99*, 391; (d) G. te Velde, F. M. Bickelhaupt, E. J. Baerends, C. Fonseca Guerra, S. J. A. van Gisbergen, J. G. Snijders, T. Ziegler, *J. Comput. Chem.*, **2001**, *22*, 931; E. J. Baerends, J. Autschbach, A. Bérces, C. Bo, P. M. Boerrigter, L. Cavallo, D. P. Chong, L. Deng, R. M. Dickson, D. E. Ellis, L. Fan, T. H. Fischer, C. Fonseca Guerra, S. J. A. van Gisbergen, J. A. Groeneveld, O. V. Gritsenko, M. Grüning, F. E. Harris, P. van den Hoek, H. Jacobsen, G. van Kessel, F. Kootstra, E. van Lenthe, D. A. McCormack, V. P. Osinga, S. Patchkovskii, P. H. T. Philipsen, D. Post, C. C. Pye, W. Ravenek, P. Ros, P. R. T. Schipper, G. Schreckenbach, J. G. Snijders, M. Sola, M. Swart, D. Swerhone, G. te Velde, P. Vernooijs, L. Versluis, O. Visser, E. van Wezenbeek, G. Wiesenekker, S. K. Wolff, T. K. Woo, T. Ziegler, ADF2004.01, SCM, Theoretical Chemistry, Vrije Universiteit, Amsterdam, Netherlands, **2004**.
[22] C. Møller, M. S. Plesset, *Phys. Rev.*, **1934**, *46*, 618.
[23] (a) R. Krishnan, J. S. Binkley, R. Seeger, J. A. Pople, *J. Chem. Phys.*, **1980**, *72*, 650; (b) A. D. McLean, G. S. Chandler, *J. Chem. Phys.*, **1980**, *72*, 5639.
[24] R. C. Binning, L. A. Curtiss, *J. Comput. Chem.*, **1990**, 11, 1206.
[25] T. H. Dunning, *J. Chem. Phys.*, **1977**, 66, 1382.
[26] A. Berger, M. Dolg, W. Küchle, H. Stoll, H. Preuss, *Mol. Phys.*, **1993**, *80*, 1431.
[27] A. E. El-Nahas, P. v. R. Schleyer, *J. Comput. Chem.*, **1994**, *15*, 596.
[28] S. Huzinaga (ed.), Gaussian Basis Sets for Molecular Calculations, Elsevier, New York, NY, **1984**.
[29] J. M. L. Martin, A. Sundermann, *J. Chem. Phys.*, **2001**, *114*, 3408.
[30] (a) R. J. F. Berger, M. Hoffmann, S. A. Hayes, N. W. Mitzel, *Z. Naturforsch.*, **2009**, *64b*, 1259–1268; (b) C. G. Reuter, Yu. V. Vishnevskiy, S. Blomeyer, N. W. Mitzel, *Z. Naturforsch.*, **2016**, *71b*, 1–13.
[31] Yu. V. Vishnevskiy, *J. Mol. Struct.*, **2007**, *833*, 30.
[32] Yu. V. Vishnevskiy, *J. Mol. Struct.*, **2007**, *871*, 24.
[33] (a) V. A. Sipachev, *Struct. Chem.*, **2000**, *11*, 167–172; (b) V. A. Sipachev, *J. Mol. Struct.*, **2004**, *693*, 235–240; (c) V. A. Sipachev, *J. Mol. Struct.*, **2001**, *567–568*, 67–72.
[34] Yu. V. Vishnevskiy, Yu. A. Zhabanov, *J. Phys.: Conf. Ser.*, **2015**, *633*, 012076.
[35] Yu. V. Vishnevskiy, D. Tikhonov, *Theor. Chem. Acc.*, **2016**, *135*, 88.
[36] M. S. Gordon, M. W. Schmidt, in *Theory and Applications of Computational Chemistry: The First Forty Years*, C. E. Dykstra, G. Frenking, K. S. Kim, G. E. Scuseria, (eds), Elsevier: Amsterdam, **2005**, pp 1167–1189.
[37] (a) R. Ditchfield, *Mol. Phys.*, **1974**, *27*, 789; (b) K. Wolinski, J. F. Hinton, P. Pulay, *J. Am. Chem. Soc.*, 1990, *112*, 8251; (c) J. Gauss, *J. Chem. Phys.*, **1993**, *99*, 3629.
[38] W. Kutzelnigg, U. Fleischer, M. Schindler, NMR Basic Principles and Progress, Springer, Berlin, **1990**, vol. 23, pp. 165–262.
[39] Same as 962(d), augmented with one set of diffuse s and p functions.
[40] (15s11p7d2f) contracted to [10s9p5d]: (a) U. Fleischer, Ph.D. Thesis, Bochum, Germany, **1992**; (b) M. Bühl, W. Thiel, U. Fleischer, W. Kutzelnigg, *J. Phys. Chem.*, **1995**, *99*, 4000.
[41] (a) A. D. Becke, *Phys. Rev. A*, **1988**, *38*, 3098; (b) J. P. Perdew, *Phys. Rev. B*, **1986**, *33*, 8822.
[42] (a) E. van Lenthe, E. J. Baerends, J. G. Snijders, *J. Chem. Phys.*, **1994**, *101*, 9783; (b) E. van Lenthe, R. van Leeuwen, E. J. Baerends, J. G. Snijders, *Int. J. Quantum Chem.*, **1996**, *57*, 281; (c) E. van Lenthe, E. J. Baerends, J. G. Snijders, *J. Chem. Phys.*, **1993**, *99*, 4597.
[43] E. van Lenthe, J. G. Snijders, E. J. Baerends, *J. Chem. Phys.*, **1996**, *105*, 6505.
[44] T. Onak, J. Tseng, M. Diaz, D. Tran, J. Arias, S. Herrera, D. Brown, *Inorg. Chem.*, **1993**, *32*, 487.
[45] M. Bühl, W. Thiel,U. Fleischer, W. Kutzelnigg, *J. Phys. Chem.*, **1995**, *99*, 4000.

Accepted Manuscript

This article is protected by copyright. All rights reserved.

10.1002/chem.201805145

WILEY-VCH

Entry for the Table of Contents

FULL PAPER

Thiole and selenole functions have been attached to icosahedral carbaboranes and their structures determined by gas electron diffraction augmented by ab initio calculated data. A method for quantifying the experimental contribution to the structural parameters has been developed and tested. Comparison of NMR chemical shifts in solution and quantum-chemically calculated ones allowed retrieving further structural information.

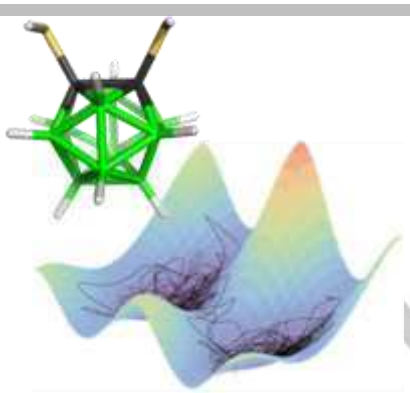

T. Baše, J. Holub, J. Fanfrlík, D. Hnyk, P. D. Lane, D. A. Wann, Y. V. Vishnevskiy, D. Tikhonov, C. G. Reuter and N. W. Mitzel*

XXX – XXX

Icosahedral carbaboranes with peripheral hydrogen-chalcogenide functions: their structures from gas electron diffraction and chemical shielding in solution

WILEY-VCH

Accepted Manuscript

This article is protected by copyright. All rights reserved.